

SUPPLEMENTARY DATA

Full Methods

Reagents

Eritoran (E5564) and its corresponding placebo (vehicle only) were kindly provided by Eisai Inc. (Japan). Eritoran was prepared at 2.33 mg/ml in sterile, endotoxin-free water and diluted for injection in sodium bicarbonate-buffered 5% dextrose water. Oxidized 1-palmitoyl-2-arachidonoyl-sn-glycero-3-phosphocholine (OxPAPC) was purchased from Hycult biotech (Plymouth Meeting, PA). *Escherichia coli* K235 LPS was prepared as previously described¹. Pam3Cys was purchased from EMC Microcollections (Germany).

Mice and cotton rats

Six to 8-week old, WT C57BL/6J, TLR2^{-/-}, and CD14^{-/-} mice were purchased (The Jackson Laboratory, Bar Harbor, ME). TLR4^{-/-} mice (provided by Shizuo Akira, Osaka, Japan) on a C57BL/6 background, were bred in UMB's accredited facility. Inbred young adult (4-8 weeks old) cotton rats (*Sigmodon hispidus*) were bred at Sigmovir Biosystems, Inc. (Rockville, MD). All animal experiments were conducted with institutional IACUC approval from University of Maryland, Baltimore and Sigmovir Biosystems, Inc.

Virus

Mouse-adapted H1N1 influenza A/PR/8/34 virus ("PR8") (ATCC, Manassas, VA) was grown in the allantoic fluid of 10-day old embryonated chicken eggs as

described² and was kindly provided by Dr. Donna Farber (Columbia University). Non-adapted human influenza virus strain A/Wuhan/359/95 (H3N2), and A/Brisbane/59/07 (H1N1) was obtained and grown as previous described^{3,4}. Non-adapted human influenza strain A/California/07/2009 strain (human pandemic H1N1) was kindly provided by Ted Ross (U. Pittsburgh).

Virus challenge and treatments

C57BL/6J WT, TLR4^{-/-}, TLR2^{-/-}, and CD14^{-/-} mice were infected with mouse-adapted influenza virus, strain A/PR/8/34 (PR8; ~7500 TCID₅₀, i.n., 25 µl/nares) or the non-adapted human pandemic H1N1 strain, A/California/07/2009 (~10⁷ TCID₅₀, i.n.). This dose was found in preliminary experiments to kill ~90% (PR8) or ~75% (human H1N1) of infected mice. Two days after infection, mice received either placebo or E5564 (Eritoran; 200 µg/mouse in 100 µl, i.v.) daily (Day 2 to Day 6). In some experiments, some groups of mice were treated with eritoran starting at day 4 or day 6 post-infection and treated for 5 or 3 consecutive days, respectively. In some experiments, some mice were infected with ~10,000 or 20,000 TCID₅₀ PR8. Mice were monitored daily for survival, weight loss, and clinical signs of illness (e.g., lethargy, piloerection, ruffled fur, hunched posture, rapid shallow breathing, audible crackling) for 14 days. A clinical score ranging from 0 (no symptoms) – 5 (moribund) was ascribed to each mouse daily⁵. In some experiments, mice were euthanized at the indicated times post-infection to harvest serum for liver enzyme levels or lungs for analysis of gene expression, lung pathology, or viral titers.

Cotton rats were infected with non-adapted human influenza strain A/Wuhan/359/95 (H3N2; $\sim 10^7$ TCID₅₀ or pfu, i.n., 50 μ l/nares). Two h post-infection, animals received E5564 (200 μ g/rat in volume, retro-orbital) daily for 5 days (days 0-4). Animals were sacrificed at day 4 post-infection for lung pathology and total RNA to measure gene expression by real time PCR.

Histopathology

Lungs were inflated and perfused and fixed with 4% PFA. Fixed sections (8 μ m) of paraffin-embedded lungs were stained with hematoxylin and eosin (H&E). Slides were randomized, read blindly, and examined for tissue damage, necrosis, apoptosis, and inflammatory cellular infiltration.

Pulse Oximetry Measurements

At 6 days post-infection, percent arterial oxygen saturation was measured on individual mice that were lightly anesthetized with nebutol. An extra small collar sensor and a Small Animal Oximetry Restraint Device (Starr-Gate, Oakmont, PA) was used per the manufacturer's instructions.

Viral titration

Virus titers were obtained from supernatants of lung homogenates of PR8-infected mice that were either left untreated (NT) or treated with Eritoran and harvested on days 2, 4, 6, and 7 post-infection and expressed at TCID₅₀/ml as described previously⁶.

Quantitative real-time PCR (qRT-PCR)

Total RNA isolation and qRT-PCR were performed as previously described⁷. Levels of mRNA for specific genes are reported as relative gene expression normalized to mock-infected lungs.

Liver enzyme levels

Serum was collected on day 7 from C57BL/6J WT mice that were either mock-infected with saline or PR8-infected and were either left untreated or treated with Eritoran (E5564) starting on day 2 post-infection. ALT and AST levels were measured using a Dimension Vista System Flex Reagent cartridge (Siemens Healthcare Diagnostics, Ltd.).

Macrophage cell cultures and treatment

Thioglycollate-elicited peritoneal macrophages from WT, TLR4^{-/-}, and TLR2^{-/-} mice were enriched as described⁸ after plating in 12-well (2x10⁶ cells/well) tissue culture plates. Macrophages were pre-treated with E5564 (10 ng/ml) for 1 h and then stimulated with LPS (10 ng/ml), P3C (300 ng/ml), or OxPAPC (20 µg/ml) for 8 h.

Matrix-Assisted Laser Desorption Ionization-Imaging Mass Spectrometry (MALDI-IMS)

Mouse lung tissue was snap frozen by floating in an aluminum foil raft on liquid nitrogen. Tissues were cryosectioned (unfixed and unembedded) in 12 µm sections, each section was transferred to a conductive MALDI-IMS glass slide, heat-fixed until visibly dry (approximately 30-60 s), and desiccated for at least 1

hour. A 12.5 mg/mL solution of norharman MALDI matrix solvated in chloroform:methanol:water (1:2:0.8, v:v:v) was spray coated onto slides using the Bruker ImagePrep device. MS data was collected in positive mode (detection range: m/z 400-900), raster width 150 μm , 500 shots per raster, on a Bruker Daltonics AutoFlex Speed Matrix-Assisted Laser Desorption Ionization Time-of-Flight/Time-of-Flight Mass Spectrometer (MALDI-TOF/TOF MS; source) using flexControl software. Subsequently, the data was analyzed using flexImaging software. After IMS analysis, the matrix was stripped in 70% methanol and tissue sections were restained by H&E for gross histological reference using standard protocols. All MALDI-IMS specific materials, equipment, instruments, and software were obtained from Bruker Daltonics (Billerica, MA). Unless otherwise specified, all reagents were purchased from Sigma-Aldrich (St. Louis, MO).

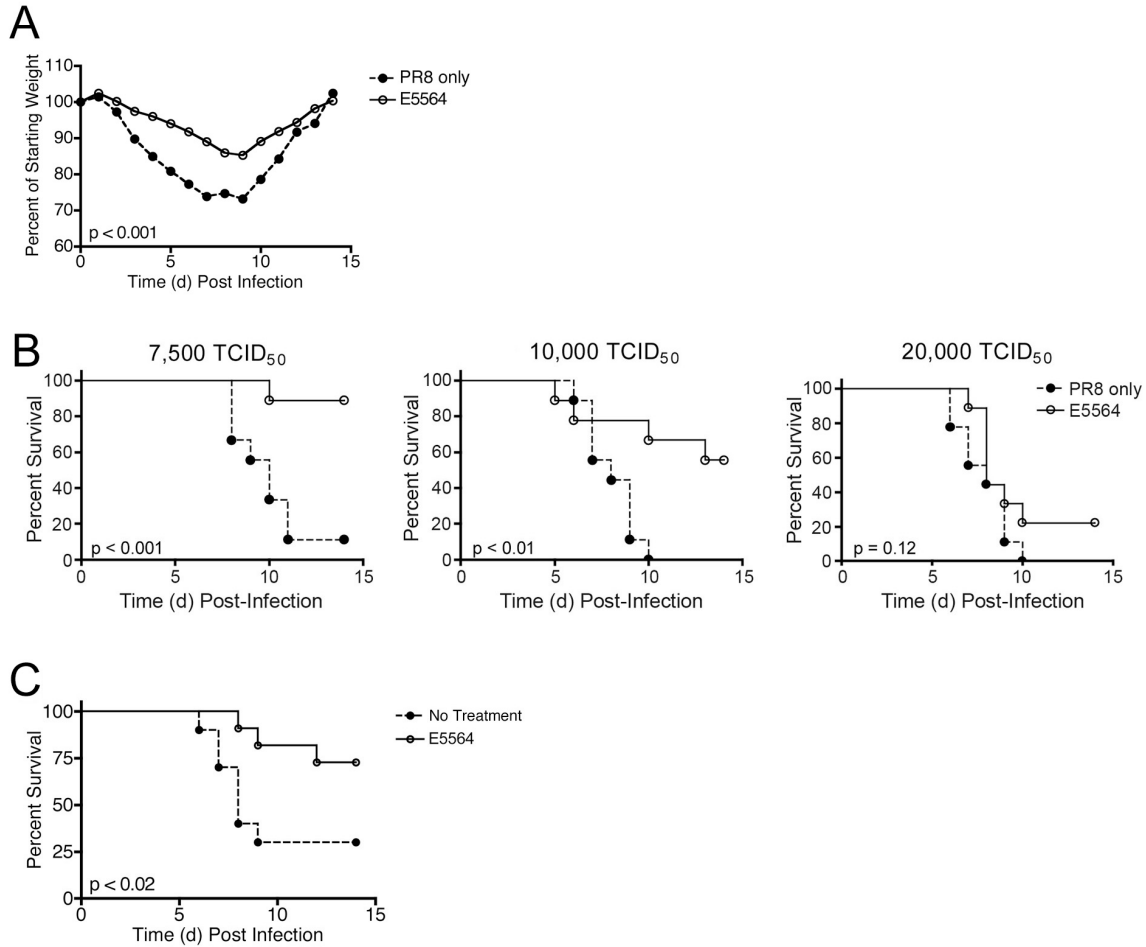
Statistics

Statistical differences between two groups were determined using an unpaired, two-tailed Student's t test with significance set at $p < 0.05$. For comparisons between ≥ 3 groups, analysis was done by one-way ANOVA followed by a Tukey's multiple comparison test with significance determined at $p < 0.05$. For survival studies, a Log-Rank (Mantel-Cox) test was used.

Supplementary References

1. McIntire, F.C., Sievert, H.W., Barlow, G.H. Finley, R.A., & Lee, Y. Chemical, physical, biological properties of a lipopolysaccharide from *Escherichia coli* K-235. *Biochemistry* **6**, 2363-2376 (1967).
2. Teijaro, J.R. *et al.* Costimulation modulation uncouples protection from immunopathology in memory T cell response to influenza virus. *J Immunol.* **182**, 6834-43 (2009).
3. Ottolini, M.G. *et al.* The cotton rat provides a useful small-animal model for the study of influenza virus pathogenesis. *J Gen Virol* **86**, 2823-30 (2005).
4. Blanco, J.C.G *et al.*, Receptor characterization and susceptibility of cotton rats to avian and 2009 pandemic influenza virus strains. *J. Virol.* **87**, 4 PMID: 2319287, (2013).
5. Tate, M.D., Brooks, A.G., & Reading, P.C. The role of neutrophils in the upper and lower respiratory tract during influenza virus infection in mice. *Respiratory Res.* **9**, 57-70 (2008).
6. Shirey, K.A. *et al.* The anti-tumor agent, 5,6-dimethylxanthenone-4-acetic acid (DMXAA), induces IFN-beta-mediated antiviral activity in vitro and in vivo. *J Leukoc Biol.* **89**, 351-357 (2011).
7. Shirey, K.A., Cole, L.E., Keegan, A.D., & Vogel, S.N. *Francisella tularensis* live vaccine strain induces macrophage alternative activation as a survival mechanism. *J Immunol.* **181**, 4159-4167 (2008).

8. Shirey, K. *et al.* Control of RSV-induced lung injury by alternatively activated macrophages is IL-4R α -, TLR4-, and IFN- β -dependent. *Mucosal Immunol.* **3**, 291-300 (2010).
9. Latz, E. *et al.* Lipopolysaccharide rapidly traffics to and from the Golgi apparatus with the toll-like receptor 4-MD-2-CD14 complex in a process that is distinct from the initiation of signal transduction. *J Biol Chem.* **277**, 47834-43 (2002).
10. Imai, Y. *et al.* Identification of oxidative stress and Toll-like receptor 4 signaling as a key pathway of acute lung injury. *Cell* **133**, 235-249 (2008).
11. Thannickal, V.J. & Fanburg, B.L. Reactive oxygen species in cell signaling. *Am J Physiol Lung Cell Mol Physiol.* **279**, L1005-L1028 (2000).
12. Morgan, M.J. & Liu, Z. Reactive oxygen species in TNF α -induced signaling and cell death. *Mol Cells* **30**, 1-12 (2010).



Supplementary Figure 1. Eritoran (E5564)-mediated protection is overcome by increased PR8 challenge doses. (A) Mice were infected (i.n.) with 7500 TCID₅₀ PR8. Mice were untreated or treated with E5564 starting on day 2 post-infection for 5 consecutive days. Mice were weighed daily. The data represent data combined from 4 independent experiments with 5 mice/treatment/experiment. (B) Mice were infected (i.n.) with either 7500 TCID₅₀, 10,000 TCID₅₀, or 20,000 TCID₅₀ PR8. Mice were left untreated or treated with E5564 starting on day 2 post-infection. Mice infected with 7500 TCID₅₀ and treated with E5564 had 100% survival, while those infected with 10,000 TCID₅₀ or 20,000 TCID₅₀ and treated with E5564 had only 75% and 25% survival, respectively. These are the

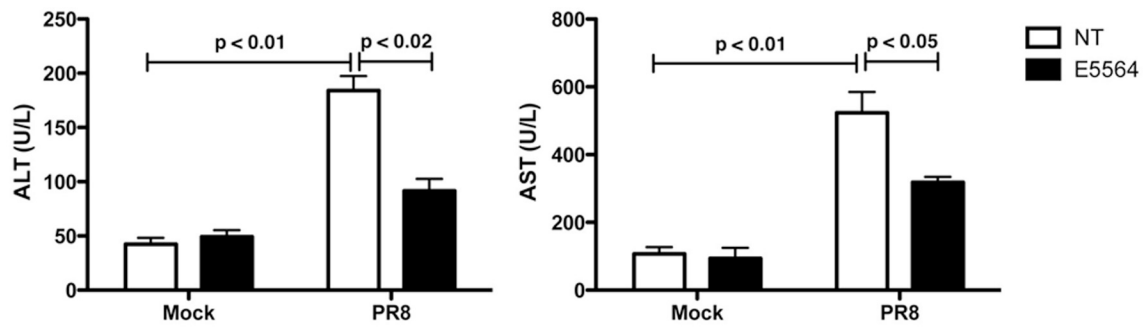
combined results from 2 separate experiments, each with 4-5 animals/ treatment group/experiment. (C) Mice were infected (i.n.) with $\sim 10^7$ TCID₅₀ A/California/07/2009 H1N1. Mice were left untreated or treated with E5564 starting on day 2 post-infection and treated for 5 consecutive days. Mice were monitored for survival for 14 days. These are the combined results from 2 separate experiments, each with 4-5 animals/ treatment group/experiment.

Table I. Eritoran is not directly antiviral^a

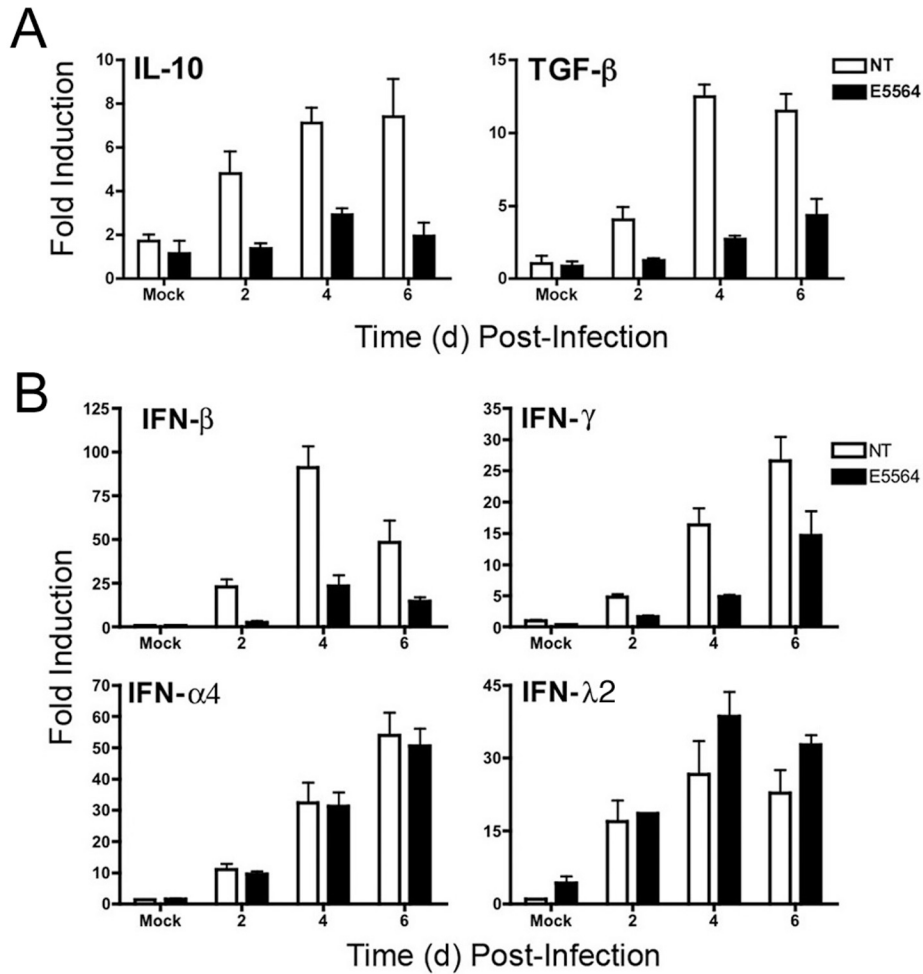
<u>A/Wuhan/359/96 (H3N2)</u>	Titer (TCID ₅₀ /ml) ± s.e.m. ^b	<i>p</i> value
Vehicle	1.2 x 10 ⁸ ± 4.9 x 10 ⁷	
E5564 treatment	5.0 x 10 ⁷ ± 2.5 x 10 ⁷	0.3
E5564 pre-treatment	5.6 x 10 ⁷ ± 2.3 x 10 ⁷	0.3
 <u>A/California/07/09 (pH1N1)</u>		
Vehicle	1.1 x 10 ⁵ ± 5.6 x 10 ⁴	
E5564 treatment	2.1 x 10 ⁶ ± 8.1 x 10 ⁴	0.5
E5564 pre-treatment	8.7 x 10 ⁵ ± 4.1 x 10 ⁴	0.5
 <u>A/Brisbane/59/07 (H1N1)</u>		
Vehicle	1.1 x 10 ⁸ ± 5.6 x 10 ⁷	
E5564 treatment	1.7 x 10 ⁸ ± 7.0 x 10 ⁷	0.3
E5564 pre-treatment	3.4 x 10 ⁷ ± 6.0 x 10 ⁶	0.3

^aVirus stocks of A/Wuhan/359/96 (H3N2), A/California/07/2009 (pH1N1), and A/Brisbane/59/07 (H1N1) were titrated in MDCK cells in the presence of E5564 (10 ng/ml) or absence of E5564 (vehicle). E5564 was applied 1 h prior (E5564 pre-treatment) or at the same time the virus was inoculated into the cell plate.

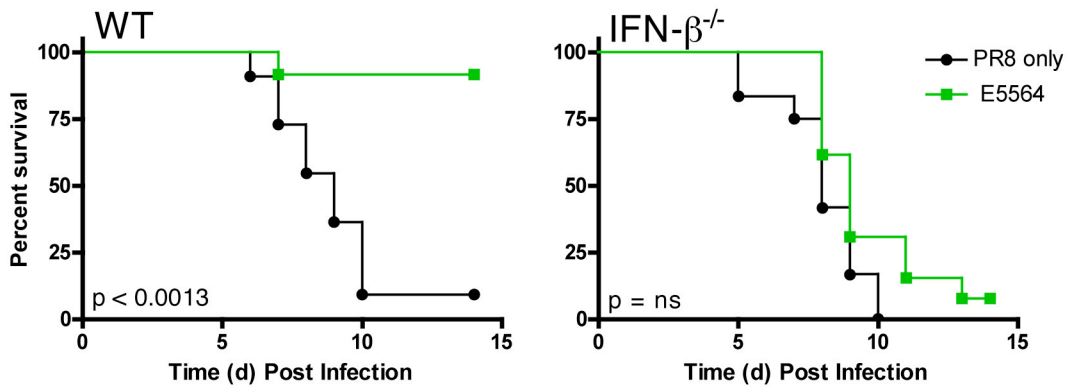
^bTiters obtained from three independent titrations.



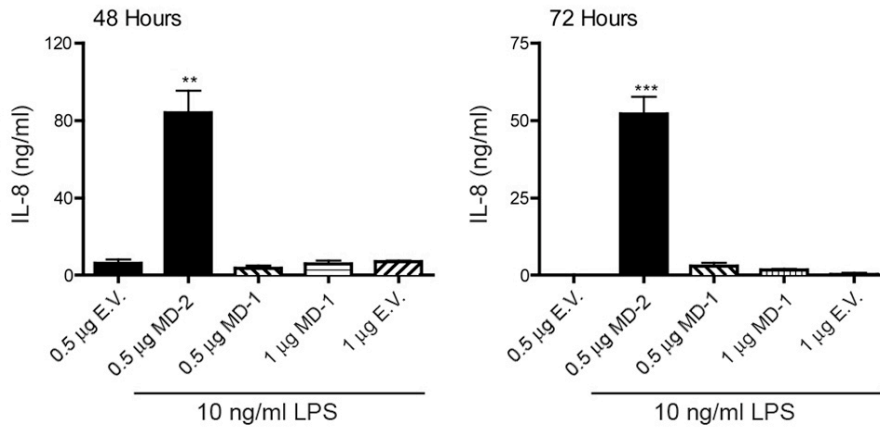
Supplementary Figure 2. Treatment with Eritoran reduces liver enzymes. Eritoran treatment blunts PR8-induced ALT and AST levels in sera. Mice were treated as described in Fig. 1A and sera harvested on Day 6 post-infection for measurement of liver enzymes. The data represent the combined results of two separate experiments \pm s.e.m. (n = 4 mice/treatment group/experiment).



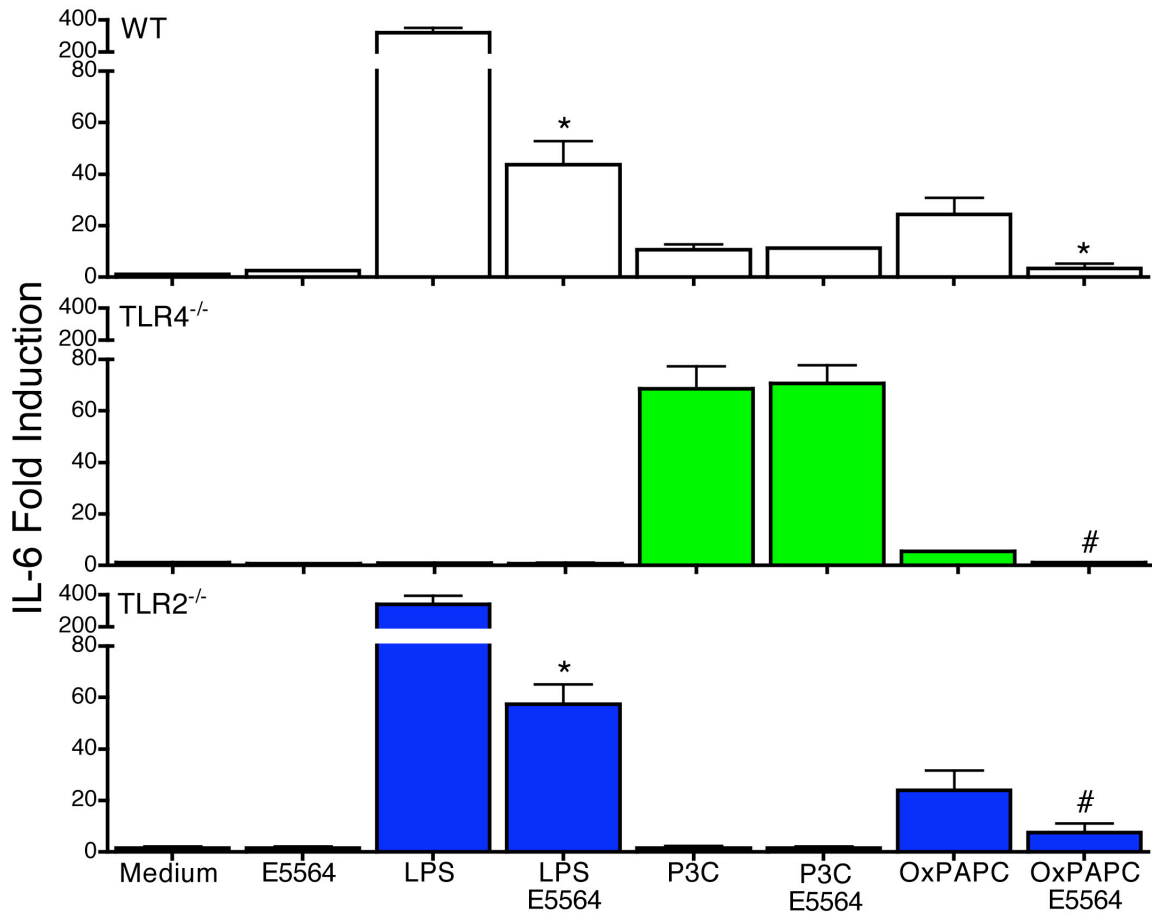
Supplementary Figure 3. Eritoran treatment suppresses influenza-induced cytokine gene expression. Mice were treated as described in Fig. 1A and euthanized on Days 2 (3 h post-treatment), 4, and 6 post-infection (4 mice/treatment group/experiment; data presented are means \pm s.e.m. from 2 separate experiments; $p < 0.01$ at each time point). Lungs were processed for total RNA and subjected to qRT-PCR for detection of specific gene expression.



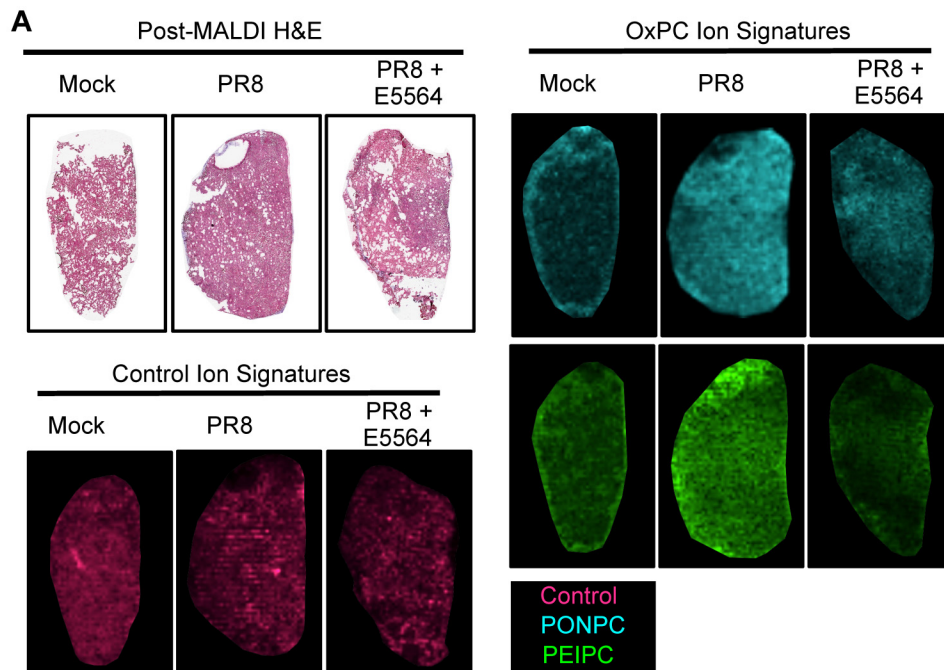
Supplementary Figure 4. Eritoran treatment does not induce protection in PR8-infected IFN- $\beta^{-/-}$ mice. WT and IFN- $\beta^{-/-}$ mice were infected with ~ 7500 TCID₅₀ PR8 and were left either untreated (circles) or treated with E5564 2 days post-infection, for 5 successive days (squares). Data represent the combined results of 2 separate experiments (6 mice/treatment/experiment; WT: untreated vs. E5564 treatment ($p < 0.0013$); IFN- $\beta^{-/-}$: untreated vs. E5564 treatment ($p = ns$)).



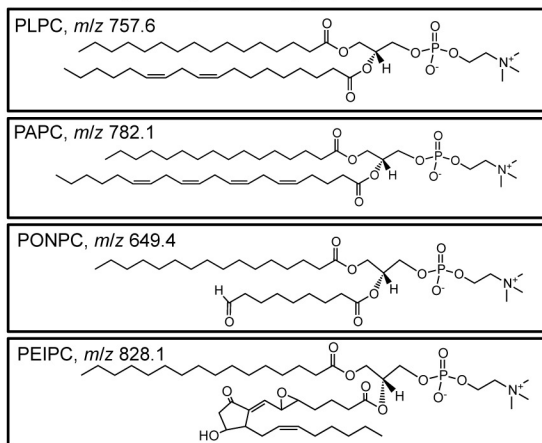
Supplementary Figure 5. MD-1 fails to substitute for MD-2 for LPS stimulation. HEK293 cells that stably express CD14 and TLR4 (HEK293-CD14-TLR4) were transfected with MD-2, MD-1 or empty vector (E.V.) as previously described⁹. At either 48 or 72 h post-transfection, the cells were mock-stimulated with PBS or stimulated with *E. coli* K235 LPS (10 ng/ml). Supernatants were collected 24 h after stimulation and analyzed for total IL-8 levels by ELISA. Data represent mean and s.e.m. of cultures in a single experiment and represent an experimental $n = 3$. (** $p < 0.005$; *** $p < 0.001$).



Supplementary Figure 6. OxPAPC signals primarily through TLR4. WT C57BL/6J, TLR4^{-/-}, and TLR2^{-/-} peritoneal macrophages were pretreated with E5564 (10 ng/ml) for 1 h and then treated with medium alone, LPS (20 ng/ml), P3C (300 ng/ml), or OxPAPC (20 μg/ml) and mRNA expression measured. Data are means +/- s.e.m. from 1 experiment with triplicate samples (* p < 0.001; # p < 0.05).

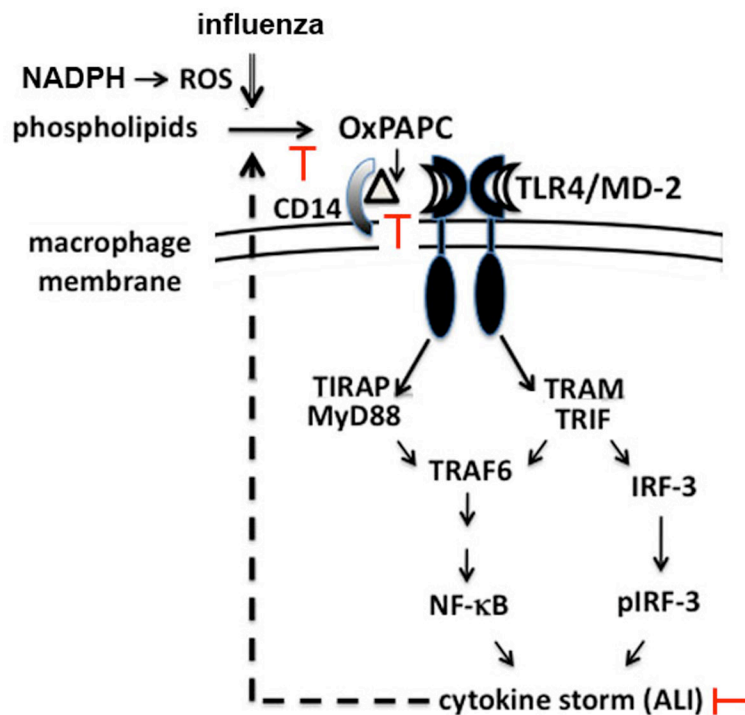


B Phosphatidylcholine (PC) Structures



Supplementary Figure 7. Detection of Lipid Ions Characteristic of OxPC. (A) Post-MALDI H&E staining of sections analyzed by MALDI-IMS (top panel). MALDI-IMS of selected lipids, positive ion mode, 150 μm raster width. Post-H&E stained tissues for reference. Left panel: control ion distribution (*m/z* 618, detection window *m/z* $\pm 0.15\%$, false color as given) (bottom panel). Right

panel: differentially detected ions (m/z 650 PONPC, m/z 830 PEIPC, m/z +/- 0.15%, false colors as given). (B) Structures of abundant phosphatidylcholine (PC) and predicted oxidized phosphatidylcholine (OxPC) molecules and molecular weights: 1-palmitoyl-2-linoleoyl PC (PLPC) m/z 757.6, 1-palmitoyl-2-arachadonyl PC (PAPC) m/z 782.1, and predicted structures of oxidized PC molecules and molecular weight, 1-palmitoyl-2-(9-oxo)nonanoyl PC (PONPC) m/z 649.4, (PEIPC) 1-palmitoyl-2-(5,6-epoxyisoprostane E2 oyl) PC m/z 828.1. Results are representative of 4 replicate experiments. In addition, predicted breakdown components were also identified at m/z 586 and m/z 680 (data not shown).



Supplementary Figure 8. Hypothetical model of Eritoran-mediated protection against influenza-induced ALI and lethality. This model is based on that originally proposed by Imai et al.¹⁰ Points in the signaling pathway at which Eritoran may block PR8-induced inflammation are indicated in red. Based on the data in Figure 5B, we would speculate that Eritoran can inhibit OxPAPC interaction with either CD14 or MD2, thus diminishing TLR4 signaling and production of cytokines (as seen in Figure 4). This, in turn, would be predicted to limit the effect of cytokines on ROS generation^{11,12} and thereby limit the oxidation of phospholipids, as observed in Suppl. Figure 5. The role of TLR2 in Eritoran-induced blockage of this pathway remains to be determined.